ENHANCING RESUNET ARCHITECTURE FOR SATELLITE IMAGE ANALYSIS: A CASE STUDY ON FOREST CHANGE DETECTION

Kavita R. Gite[1], Dr. Praveen Gupta[2]

[1]Ph.D Scholar CSE, CSMU Panvel College

[2]H.O.D Dept. of CSE and IT, CSMU Panvel College

ABSTRACT

When looking for changes caused by forest catastrophes, it is best to employ an object-based approach in combination with High Resolution (HR) satellite pictures. By using a method similar to the initial calibration procedure, an automated feature selection strategy is used to enhance image segmentation. A multitemporal classification in view of a clever descriptor that relies upon the level of fracture of the recognized locales makes the partition of wind-tumble from unblemished regions possible. Along with the classification approach, the segmentation process also made use of the mean shift method. Beginning testing of the technique was directed utilizing a high-goal Formosat-2 multispectral satellite picture pair obtained before to and after to the Klaus storm. Positive outcomes were seen, and the meaning of high-goal pictures in the planning of woods calamities is examined.

Keywords: multitemporal classification, segmentation, feature selection, change detection, forest damage

I. INTRODUCTION

Wind storms are becoming more frequent due to the ongoing effects of climate change. Quick mapping of wind-fall damages is necessary for fire prevention, compensation claims, and updating the national forest inventory. While fallen trees make ground investigations more difficult, remote-sensing equipment can swiftly monitor large, inaccessible areas. The increased geographical and temporal precision of current satellites have greatly increased their use for disaster change detection on a global scale. In this study, we binary map areas that have been harmed and those that have not using HR satellite images of two 8-meter-resolution multispectral Formosat-2 photographs. These images were taken on January 24, 2009, in the southwest of France, both before and after the Klaus Storm.

Prior research on clear-cuts in forestry relied on hectare-scale, low-resolution maps. Research on small structural changes, such as wind-fall damage, is limited. New forestry modifications were detected using object-based classifiers [1][2]. To order pixels utilizing new article descriptors, these strategies first utilize spatial and ghastly data to divide them into homogeneous zones. [3] or spatial and textural [2].

One way to discover changes is by analysing multi-temporal photographs or by comparing storm classifications before and after the event (post-classification). Although post-classification algorithms provide trustworthy

"from-to" change information and are strong to radiometric changes across pictures (Im and Jensen, 2005), errors may still spread. Additional information regarding minute alterations is provided by joint classification. Thresholding in view of a parametric measurable test [2] master information, or AI utilizing a preparation set [4] are potential methodologies.

Storm damage at a fine geographical scale may be mapped using the proposed object-based, multi-temporal classification. Our method for fast regional mapping is almost entirely automated and uses very little data. Rather than post-classification, we opted for unsupervised multi temporal classification since it's hard to see subtle changes in a single after-storm image. As mentioned in Section 2, the method relies on Mean Shift Segmentation. To improve image segmentation, Section 3 introduces a novel automatic feature selection method that is similar to calibration. Binary multi-temporal classification using a new area-fragmentation-based descriptor is introduced in Section 4 using the mean shift technique. The outcomes and conversation of the tests are introduced and talked about in Segment 5.

II. REVIEW OF LITERATURE

Recognizing changes in satellite pictures [20] is now an absolute must for understanding global environmental change, resource surveys, and urban planning. In contrast, a plethora of satellite images were steadily acquired every second, serving as a vital resource for the assessment of the spatiotemporal situation. In addition, it is still a major challenge to get reference data for satellite images that account for changes in the quantity of land covered. Standard approaches for changed detection were also made worthless by the intricacy of texture features.

To get beyond these limitations, a practical approach to modified detection was laid forth. Fuzzy neural network (FNN) classification, which blends fuzzy logic with NN, and generative adversarial network (gan) segmentation based on Taylor Shuffled Shepherd Optimisation (Tsso) were both used. The proposed tsso is the result of merging the Taylor series with shuffling shepherd optimisation (sso). At its peak, it achieved a kappa coefficient of 0. 911, an overall error of 0. 0704, and an accuracy of 0. 932. With respect to accuracy for image-1, the constructed tsso-based gan + fuzzy nn surpassed the aforementioned networks by 2.28%, 4.78%, 0.33%, and 13.16%, respectively. The networks in question were ppcnet, ifn, multiclass support vector machine, kernel principal component analysis convolutional mapping network, and patchlevel and pixel-level changed detection network.

III. METHODS

A. *Area of study and data references*

Figure 1 shows the locations of the five quadrat study sites in Tuscany that were chosen at random to cover a total of 4,600 hectares. The regions were built by arbitrarily choosing five woods packages in Tuscany as the quadrat focuses. As indicated by the Regione Toscana (2003/08/08, n.48\R), the maximum permissible size for coppiced and clearcut forests in the study area is 20 hectares.
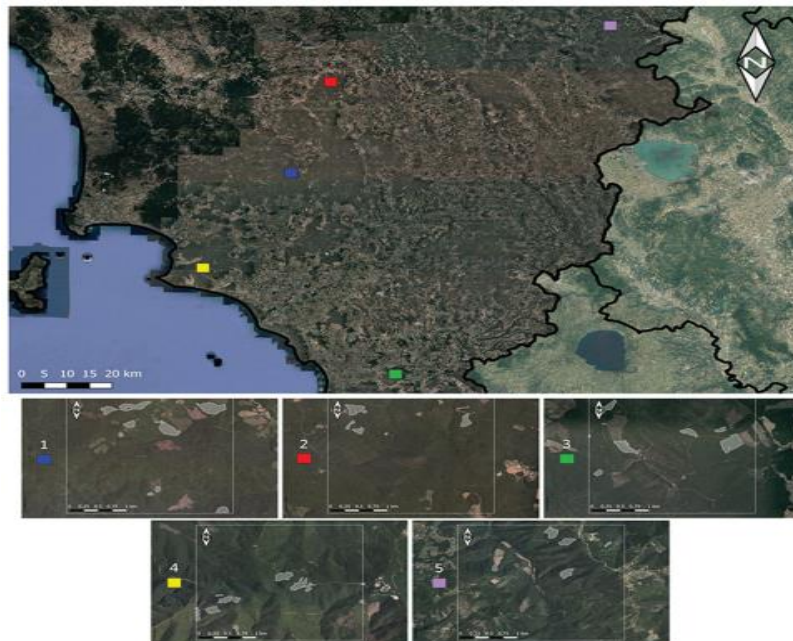
Figure 1. Located at the top are the five research areas, and plotted out at the bottom are the reference clearcuts for each of those areas(5).

For each site, we delineated previously logged, non-forest, and temporarily unstocked regions. In this study, we used 3,783 hectares (ha) of the 4,450 hectares (or on the other hand 97% of the all out region) that were covered by backwoods.

Using this method and [5], a reference geodatabase was generated. With the help of the local forest authorities, we documented every disturbance to the forest from 1 September 2018 to 5 July 2019, with the exception of damage caused by wind and forest fires. Area one had ten clear cuts covering thirty-two hectares, area two had six, area three had twenty-four, area four had fifteen, and area five had five. A total of forty-two vector polygons, or 88 hectares, were retrieved from the reference geo database. For reference mapping, we relied on photo interpretation of Planet Scope photos. After that, we field verified all of the reported polygons. We were able to get a reference geodatabase that was based on census data that was error-free. At random, we selected one spot (the blue region in Figure 1) to calibrate our algorithm and four more to test and assess the technique.

B. Planet Scope imagery

According to [6], we only used publicly available, free Planet Scope photographs online for photointerpretation and automated technique development. The Planet Tile Administrations (https://developers.pla net.com/docs/basemaps/tile-administrations/) gave everyday admittance to the 8-digit RGB apparent range groups. The photographs were downsized from 3 megapixels to 3.46 megapixels after the geometric co-registration process. According to [15], images were discarded if their valid pixel count fell below 70%. There are still valid images (VI). In order to filter out the clouds (pixels with digital numbers more than 184) and the shadows (pixels with values less than 33), a mask was made for every single picture. From May 1, 2018, to July

5, 2019, a total of 572 GeoTIFF photographs were added to the geo database (Figure 2), with 99 photographs for region 1, 124 for region 2, 100 for region 3, 77 for region 4, and 172 for region 5 caught.

All strategies for pre-elaboration were executed utilizing the open-source JavaScript bundle [9]. We looked at a lot of indices that use visible band data to separate disturbed areas in images from undisturbed ones in order to detect forest change. The "best" index was selected by photointerpreting the index with the most distinct clearcuts after calculating many indices over the starting area from the remote sensing List Information base (https://www.indexdatabase.de/). We choose the Hue index (eq. 1) from the following URL: https://www.indexdatabase.de/ db/i-single.php?id=34.
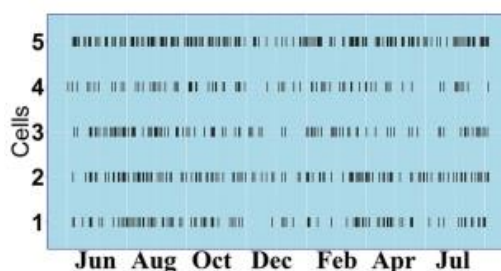

Figure 2. When were the pictures acquired?(7)

$$Hue_{idx} = arctg\left(\frac{2Red - Green - Blue}{30.5}(Green - Blue)\right)$$

While concentrating on the corruption of dry common habitats in Tunisia [10] and Nepal [11], specialists utilized Hueidx, with a marginally changed equation, to gauge the natural matter substance of soil to support soil ripeness the executives measures. We don't have the foggiest idea how it responds to otherworldly shift from non-obvious causes, for example, consumed regions and windstorm harm, and it has never been utilized to plan timberland change.

Mists had a lot of lower Hueidx values than crops, as opposed to the Standardized Consume Proportion (NBR) record [12]. This component decreases the impact of mists in photos. With no extra mistakes presented by the cloud expulsion technique, the quantity of substantial perceptions utilizing even pixels to some extent darkened by genuinely thick mists expanded.

C. Normalization

Normalization is essential when using optical sensor photos for time series analysis, since they may have been shot in different lighting conditions [6]. We used the soft max function (eq. 2) to normalise each image pixel, Huepx, where the denominator term is the amount, everything being equal. We were unable to find any references for remote sensing image nor malization, anyway the softmax capability is a notable information mining nor streamlining technique [13]. A stack of normalised pixels with values ranging from 0 to 1 is present in each area. This stack will be referred to as the Softmax Normalised Images Stack from here on out.

$$softmax(px) = \frac{e^{Hue_{px}}}{\sum e^{Hue_{px}}}$$

D. The algorithm for categorization

Reward and Penalty for Thresholding According to Hammoudeh [14] and Wiering et al. [15], TRP is based on reinforcement learning techniques. Each image in PlanetScope is examined separately, and pixels are either a "reward" or a "penance" depending on whether they saw a clearcut or not. Instead of using the reference dataset used in supervised learning, an image threshold is used to determine rewards and punishments. A pixel is rewarded if the SNS change value is higher than the threshold; else, it gets punished. As their rewards get closer to a goal, pixels transform into forest changes. In this case, the system's "memory" refers to pixel histories. In the Memory Layer, we carried it out. We outlined the TRP workflow below and in Figure 3.

In social media images, pixels depicting forest changes exhibited greater normalised Hue index values compared to pixels depicting stable forests. Pictures of clearcuts with dense clouds above them are meaningless. Hue index noise, which may lead to com mission errors, can be caused by environmental factors and fluctuations in seasonal light angles. With the help of TRP, we were able to improve the signal-to-noise ratio and remove these inconsistencies from the forest change map, making it more dependable with each new photo that comes from PlanetScope.

The engineered time series ΔSNS is created by TRP by looking at the Tint file of the I-th picture (SNSi) to the middle (s) of the appropriation of Tone records from May-August 2018 (eq. 3), which is the leaf-on season for the deciduous trees that were dissected. As our reference clearcuts began in September, we guessed that they would start around the same time.
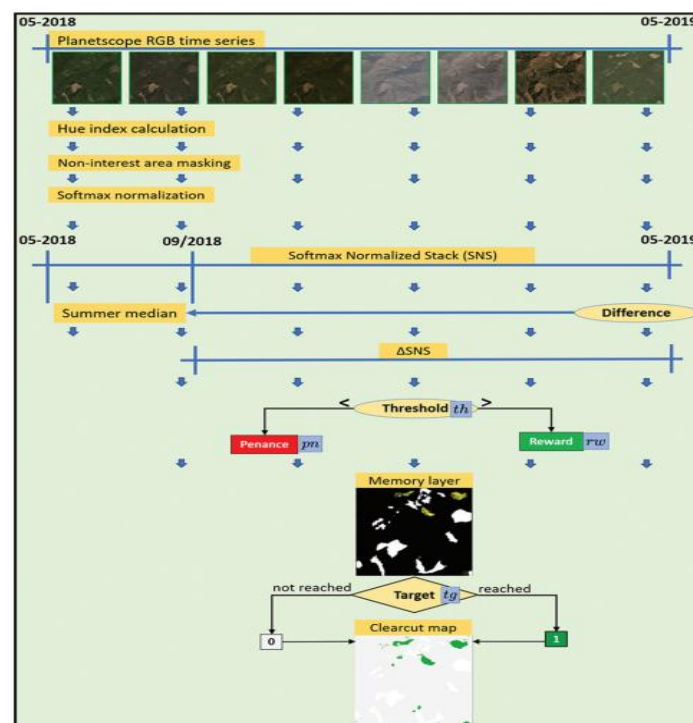

Figure 3. Workflow in TRP(7).

$$\Delta SNS_i = SNS_i - s$$

Absolute values of SNSi-s are low for pixels that were not changed from the previous summer in ŚSNSi, but they are high for pixels that were changed in the forest, assuming that low light or cloudy conditions do not affect them.

Three parameters are input to TRP: for ΔSNS, the value ranging from 0 to 1 is the threshold. There is a range of -1 to 0 for the penance, and there is a possibility that the aim is more than 1. The ΔSNS time series applies the threshold th to every image. For each pixel value greater than th, one is added, while for each pixel value lower than th, pn is subtracted as penance. A fresh Memory Layer (ML) raster image is generated for the purpose of computing and recording penances and rewards for each Planet Scope picture once it has been examined. Lastly, forest change only occurs for ML pixels with tg values. Figure 4 depicts the classification scheme.

E. Optimization

To get the most out of the method, you need to discover the values of the th, pn, and tg parameters that maximise the MCC (Matthews, 1975).

$$MCC = \frac{(TP * TN) - (FP * FN)}{\sqrt{(TP + FN) * (TP + FP) * (TN + FN) * (TN + FP)}}$$

the sum of all possible outcomes, including positive and negative results as well as false positives and negatives. We used reference data for one of the five locations to heuristically look for the ideal blend of the three boundaries; to ensure that the model was generalizable and avoid overfitting, we used the other four areas for independent validation. A hundred different permutations of the following parameters were used to test the method: th = 0.1-0.4, pn = -0.2-0.8, pf = 0.15, and tg = 1.5-6.5. We established the parameter range based on our algorithm knowledge and early research.

F. TRP performance assessment

Execution of TRP was assessed utilizing four approval regions taken from a different dataset. Table 1 displays the results of the confusion matrix study for both the user and the producer in terms of accuracy. A total of three values were used to calculate the CC and compare it to the forest areas. Complete CC and Timberland regions were determined utilizing reference information. We use a reference dataset based on the census, which is assumed to be error-free, consequently these CC and Timberland region values are right. Following that, we added up the area of the CC and Forest maps. Although these estimations—also known as pixel counting— are natural, they are one-sided because of the way that they don't represent grouping mistake. Third, the fair separated CC class region assessor from Olofsson et al. [8] was utilized.
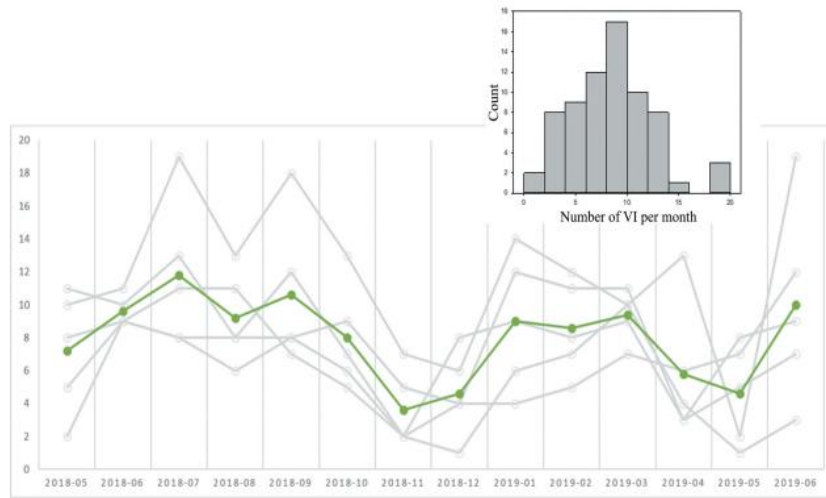
Figure 4. Green represents the average throughout the five locations, and the availability of PlanetScope VI during the research period in each area and month is also shown. You can see the monthly and area-specific VI histogram in the top right corner(8).

Table 1. Confusion matrix.

Map class	Reference class		Total	User's accuracy	$\hat{p}_h$	
	CC	Forest				
CC	$n_{11}(TP)$	$n_{12}(FP)$	$n_{1\cdot} = n_{11} + n_{12\cdot}$	$ua_1 = \frac{n_{11}}{n_{1\cdot}}$	$\hat{p}_1 = \frac{n_{11}}{n_{1\cdot}}$	$\widehat{Var}(\hat{p}_1) = \left(1 - \frac{n_1}{N_1}\right) \cdot \frac{\hat{p}_1 \cdot (1-\hat{p}_1)}{n_1}$
Forest	$n_{21}(FN)$	$n_{22}(TN)$	$n_{2\cdot} = n_{21} + n_{22}$	$ua_2 = \frac{n_{22}}{n_2}$	$\hat{p}_2 = \frac{n_{22}}{n_2}$	$\widehat{Var}(\hat{p}_2) = \left(1 - \frac{n_2}{N_2}\right) \cdot \frac{\hat{p}_2 \cdot (1-\hat{p}_2)}{n_2}$
Total	$n_{\cdot1} = n_{11} + n_{21}$	$n_{\cdot2} = n_{12} + n_{22}$				
Producer's accuracy	$pa_1 = \frac{n_{11}}{n_{\cdot1}}$	$pa_2 = \frac{n_{22}}{n_{\cdot2}}$				

\# N_h is the total number of map units in the hth map class

$$\hat{A}_{CC} = A_{tot} \cdot (wt_1\hat{p}_1 + wt_2 \cdot \hat{p}_2)$$

with standard error

$$SE(\hat{A}_{CC}) = A_{tot} \cdot \sqrt{wt_1^2 \cdot \widehat{Var}(\hat{p}_1) + wt_2^2 \cdot \widehat{Var}(\hat{p}_2)}$$

Where Atot signifies the general region, wt1 means the level of the whole region in the CC guide class, bp1 and bp2 signify the extents of reference CC perceptions in each guide class, and the recipe is seen as in Table 1. The Forest class area estimator is similar to the CC map class, except that it uses the Forest map class to calculate ^p1 and ^p2. Table 1 shows that 500 pixels were randomly selected from both the clearcut and undisturbed forest portions of the map (n1 = n2 = 500 pixels), which led to the third result. We produced a 1000-point sample from the anticipated clearcuts map even though we had a reference dataset based on the census. Separated inspecting was utilized since the example sizes would have been excessively minuscule for the CC guide class utilizing straightforward irregular or methodical testing with an obliged CC guide region. In the absence of a reference set based on a census, this stratified sample-based estimator proves to be efficient.

IV. RESULTS AND DISCUSSION

A. Research domain and dataset

French Atlantic coast is where you'll find the Nezer forest. The pine trees there are uniform in size and age, and they form rectangular stands. Figure 5 shows ortho-redressed, geo-referred to multispectral Formosat-2 pictures taken on December 22, 2008, and February 4, 2009, separately, when the Klaus storm. Each of the four of the noticeable and close infrared light ranges are found in the 8-meter pictures. Ancillary data includes tree stand delimitations, ages, a GIS layer, and one hundred reference areas on fifteen centimetre orthophotos taken on February 26, 2009.
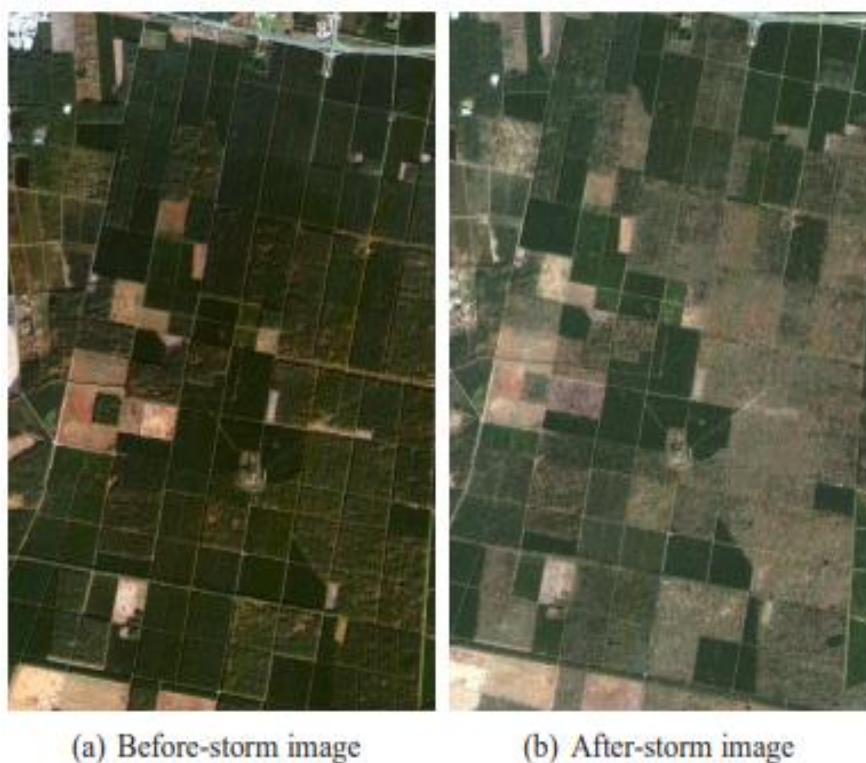

(a) Before-storm image   (b) After-storm image

Figure 5: Before and after the Klaus storm, formosat-2 took multispectral pictures(16).

B. Use of Features in Classification and Segmentation

You may find the input characteristics for spectral, textural, and temporal data in Table 2. Using the six spectral features as a basis, it calculates three temporal characteristics and ten textural features, for a total of eighty-four features. As an experimental adjustment for textural qualities, the local range and directional vector counterbalances were set to 1 pixel, and the uprooting vector was level.

These elements were utilized in highlight determination either alone or in a multi-highlight test outline after standardization. A test outline with four districts was utilized. The spatial span hs utilized for MS division depended on earlier subjects' information on thing size. A standard forest pattern is a 3-pixel zone, thus that's why hs was set to 3. To determine the radiometric range hr, we automatically optimised the Mean-Shift parameters by rescaling each feature from 0 to 255 and then testing spectral ranges from 2 to 60.

Table 2: Input features

Spectral	Textural	Temporal
Blue	Mean	Difference
Green	Variance	Ratio
Red	8 Haralick features:	Mean correlation
PIR	mean, contrast, entropy	
NDVI	Angular Second Moment	
SAVI	Inverse Difference Moment	
	Sum average, Sum entropy	
	Sum variance	

In order to detect minute changes, the MS spectral classification made use of the narrowest spectral range, hr=2. Instead of MS division, this otherworldly put together gathering stage depends completely with respect to the transient highlights of items. They were created by averaging the worldly elements across the separated after-storm zones. The best attributes and phantom reaches for picture division and arrangement are displayed in Tables 3 and 4.

Table 3: Using a test frame of four samples, determine the best features and spectral ranges for both the before- and after-storm segmentations. To review, Eq. 1 states that SP is the segmentation performance.

After-storm segmentation			Before-storm segmentation		
Feature	h_r	SP (%)	Feature	h_r	SP (%)
Red Ratio	17	87.2	Red	2	80.7
Red	3	78.1	NDVI	3	77.3
Green Ratio	16	75.5	Green	5	68.7

Table 4: Using a 4-sample test frame with hr=2, what attributes are most useful for binary classification?

Feature	SP (%)
Green Difference	92.6
NIR Difference	70.5
Red Difference	64.5

For this kind of study, spectral or tem poral characteristics work well. It is expected that 2m panchromatic photos would enhance the performance of textural characteristics. It is challenging to use textural information, particularly in forestry, utilizing the extremely low spatial goal (8m) of Formosat-2 multispectral pictures. Small windows (3×3), on which the Haralick characteristics were processed, may not have done a good job of capturing the stand texture. Maximal textural features may also result from fractured stems oriented in the same direction. Therefore, optimising the Haralick parameters and increasing the resolution should help texture characteristics.

Tem poral works well for segmentation after a storm. The level of progress consequently is impacted by the stand structure, which relies upon tree age, before the tempest. The spectral ranges provided by temporal characteristics are also larger than those of image bands. Since time-related attributes follow a normal distribution, a wide spectrum may divide the image into clear levels of change. A narrower range is required to distinguish between minute changes, however, since the initial picture bands are more varied. We looked at many feature segmentations. Based on our experimental results, single-feature segmentation is the superior method. This unexpected result may be attributed to two things. Initial, a solitary ghastly reach hr is utilized for various viewpoints in Mean Shift (Co maniciu and Meer, 2002). Its most memorable execution zeroed in on sectioning grayscale and variety pictures. Versatile ghostly reach per component could upgrade results since remote detecting photographs contain different otherworldly circulations of picture groups. Second, damage is only one of several variables that affect the complexity and diversity of forest canopies. According to Orny et al. (2010), there was a 5% drop in worldwide grouping exactness when the eight starting groups (from when tempest photos) were utilized for division in the conventional way.

C. Division and rate of fragmentation

As shown in Figure 6, the best features were used for pre- and post-storm segmentation. Some parts may be destroyed, while others may be unharmed. In contrast to undamaged regions, which are wider and share boundaries in both segmentations, dammed landscapes are more fragmented and have more little portions.
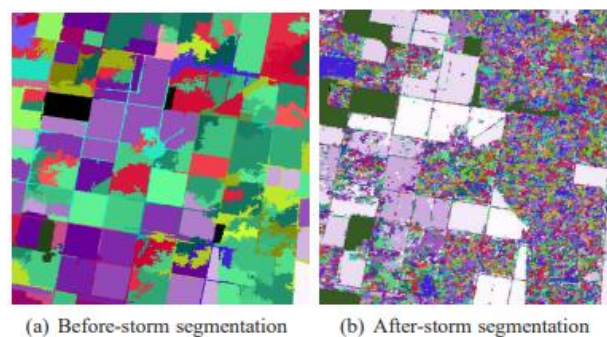

(a) Before-storm segmentation   (b) After-storm segmentation

Figure 6: Red band and red band ratio are the best characteristics for picture segmentation before and after a storm, respectively(18).

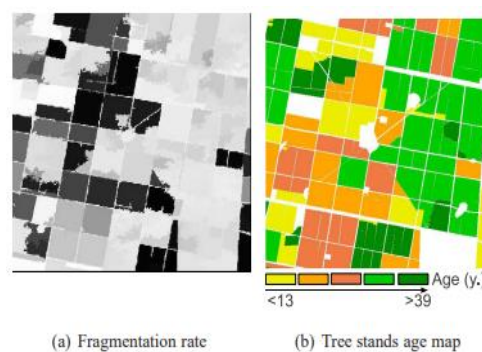(a) Fragmentation rate   (b) Tree stands age map

Figure 7: A study comparing the ages of tree stands with the rate of fragmentation(18).

You can see the gray-level segment fragmentation rate (FR) before the storm in Figure 7. Damage is more severe on lighter areas. Damage is more pronounced in older stands compared to younger ones, as seen on the tree stand age map. Wind sensitivity is affected by a number of factors, one of which being the height of the trees. A young stand is more resistant to wind because it contains numerous little trees. Sylvicultural practices have resulted in decreased density and more heterogeneity in older stands, which in turn have higher trees that are more susceptible to storm damage.

Figure 8 displays the clusters of MS spectral classifier change. It leads to about 30 clusters of changes. The histogram complexity of this image makes automated cluster classification challenging. On the other hand, you can tell damaged areas apart from undamaged ones by looking at their average fragmentation rate.
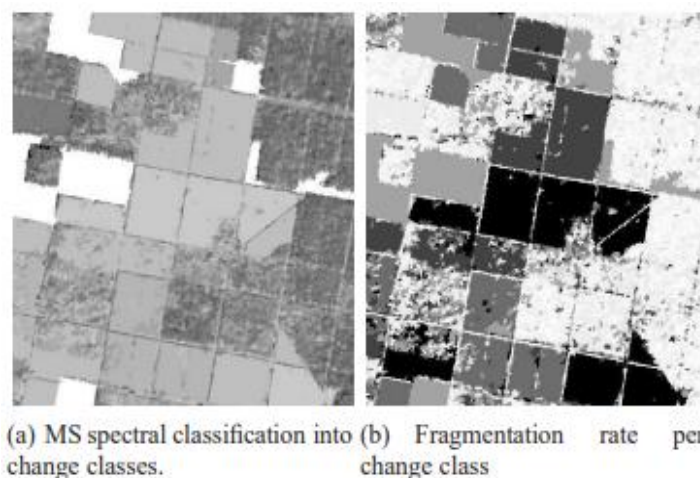

(a) MS spectral classification into change classes. (b) Fragmentation rate per change class

Figure 8: Segmentation rate and MS spectral categorization

D. Map validation

The finished binary map for forest catastrophe detection, depicting damaged and undamaged zones, is shown in Figure 9. Referential data were gathered from 15 cm orthophotos taken after the storm. Table 5 shows the worldwide disarray network, which is the result of comparing the pixel values of the reference data with the classification results.

Table 5: Matrix for confusion-free binary categorization of "in tact" or "damaged"

	Reference data		Total
	Intact	Damaged	
Intact	1390	487	1877
Damaged	80	2471	2551
Total	1470	2958	4428
Omission error	5.44	16.5	
Commission error	25.9	3.14	
Global accuracy	**87.2**		

The total accuracy rate was 87.2%. The restricted spatial goal of Formosat-2 forestalled the recovery of specific little changes or entire regions. Segmentation is vulnerable to changes in shadows since our approach does not account for them.

The INRA 1 stock information layer for the Nezer site incorporates the times of every backwoods stand. The categorization was a challenge. Error and damaged pixel rates were used to determine all ages. Pictured below are the results.

As the class becomes older, the accuracy of the classification improves dramatically. There is a correlation between tree height and wind sensitivity [18]. Older stands have a higher damage rate, reaching 70% for those older than 25 years.

Excellent identification accuracy (93.3-99.4%) was seen in individuals aged 14–39 (four intermediate classes).According to Table 5, the detection rates were lower and the number of omission and commission errors was higher for the oldest and youngest stands, respectively. Old, sparse stands of trees are mistaken for damaged areas. It may be difficult to see small damage areas or sagging trees in young, dense groups.

Figure 9: Binary map of wind storm damaged area(19).

You may compare these results to the supervised object-oriented work on 10m high-resolution multi-spectral photos done by Schwarz et al. [19]. Our accuracy (87.2%) using an automated object-based technique is lower than the 96% reported by Schwartz et al. [19]. The classification accuracy was somewhat higher (96% vs. 95%) for trees that were 14–39 years old. Classes that are advanced or older tend to fare better. Previous comments made it clear that younger classes do struggle. A small number of samples are all that is required to construct the test frame and fine-tune our method's two parameters. When it comes to emergency mapping, less time spent training and adjusting is required.

V. CONCLUSION

This study presented a new method for emergency mapping that uses object-based multi-temporal change detection. There are two main ways in which our contribution differs from conventional forestry practices. One new approach to automatic feature selection for classification and segmentation makes use of test frames (single or multi-bands) that include appropriate forest samples. This innovative feature selection method promptly assesses hundreds of attributes and combined features, drawing inspiration from camera calibration. Whether you're working in forestry or not, it may enhance your segmentation approach. Our second new development is a fragmentation rate that is tailored to storm damage and can automatically transform clusters into a binary map using thresholds. We are pleased with the results of our method. Since it needs little supervision and simply a small number of samples to construct test frames, it is categorised as unsupervised. Our method for detecting changes uses just two parameters that the user specifies and does not rely on any statistical assumptions, all because of the robust Mean-Shift clustering algorithm.
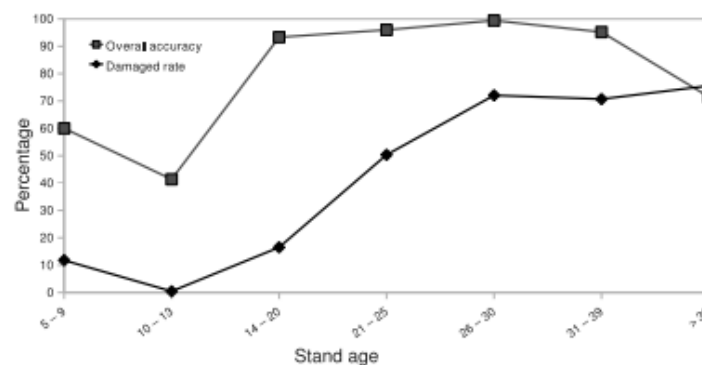

Figure 10: The rate of damaged pixels and the accuracy of classification according to age groups.

Formosat-2 multispectral images could not be enough for finding dispersed little damage because of their low spatial resolution (8m). When it comes to forests in particular, this resolution is woefully insufficient for making good use of textural information. It is possible that 2m panchromatic photos may enhance the current mapping performance. Lastly, the age class map and the binary (intact/damaged) classification were in agreement, proving that the wind sensitivity of the tree increased with age.

In the end, we need to apply our change discovery technique to panchromatic and extremely high-goal pictures of the Nezer site. To better detect minute changes and capture textural forest traits, a higher spatial resolution is required. When dealing with early thick stands, hierarchical approaches might be useful for spotting subtle

changes. To make the most of the diversity in spectral distribution and the abundance of features, the Mean Shift technique should additionally adjust the spectral range hr for each feature.

REFERENCES

[1]. Conchedda, G., Durieux, L. and Mayaux, P., 2008. An objectbased method for mapping and change analysis in mangrove ecosystems. ISPRS Journal of Photogrammetry and Remote Sensing 63(5), pp. 578–589. Theme Issue: Remote Sensing of the Coastal Ecosystems.

[2]. Desclee, B., Bogaert, P. and Defourny, P., 2006. Forest change detection by statistical object-based method. Remote Sensing of Environment 102(1-2), pp. 1–11.

[3]. Fraser, R., Abuelgasim, A. and Latifovic, R., 2005. A method for detecting large-scale forest cover change using coarse spatial resolution imagery. Remote Sensing of Environment 95(4), pp. 414–427.

[4]. Im, J. and Jensen, J., 2005. A change detection model based on neighborhood correlation image analysis and decision tree classification. Remote Sensing of Environment 99(3), pp. 326–34

[5]. Chirici, G., Giannetti, F., Mazza, E., Fancini, S., Travaglini, D., Pegna, R., & White, J. C. (2020). Monitoring clearcutting and subsequent rapid recovery in Mediterranean coppice forests with Landsat time series. Annals of Forest Sciences, 77(2). https://doi.org/ 10.1007/s13595-020-00936-2

[6]. Leach, N., Coops, N. C., & Obrknezev, N. (2019). Normalization method for multi-sensor high spatial and temporal resolution satellite imagery with radiometric inconsistencies. Computers and Electronics in Agriculture, 164, 104893. https://doi.org/10.1016/j.com pag.2019.104893

[7]. Wiering, M., Van Hasselt, H., Pietersma, A.-D., & Schomaker, L. (2011). Reinforcement learning algorithms for solving classification problems. Institute of Electrical and Electronics Engineers. https://doi.org/10.1109/ ADPRL.2011.5967372.

[8]. Olofsson, G. M., Foody, M. H., Stehman, S. V., Woodcock, C. E., & Wulder, M. A. (2014). Good practices for estimating area and assessing accuracy of land change Pontus. Remote Sensing of Environment, 148, 42–57. https://doi.org/10.1016/j.rse.2014.02.015

[9]. Cheng, J., Karambelkar, B., & Xie, Y. (2018). Leaflet: Create interactive web maps with the javascript 'Leaflet' library. The Comprehensive R Archive Network (CRAN).https:// CRAN.R-project.org/package=leaflet.

[10]. Escadafal, R., Belghith, A., & Ben Moussa, H. (1994). Indices spectraux pour la dégradation des milieux naturels en Tunisie aride. CNES.

[11]. Mandal, U. K. (2016). Spectral color indices based geospatial modeling of soil organic matter in Chitwan District, Nepal. International Archives of the Photogrammetry, Remote Sensing and Spatial Information Sciences - ISPRS Archives, 41, 43–48. https://doi.org/10.5194/isprsarc hives-XLI-B2-43-2016

[12]. Key, C. H., & Benson, N. C. (2006). Landscape assessment (LA): Sampling and analysis methods. USDA forest service Gen. Tech. Rep RMRS-GTR-164–CD. https://www.fs. usda.gov/treesearch/pubs/24066

[13]. Torgo, L. (2016). "Data mining with R learning with case studies. Chapman and Hall/CRC. https://doi.org/10.1201/9781315399102

[14]. Hammoudeh, A. (2018). A concise introduction to reinforcement learning. https://www.researchgate.net/publication/ 323178749_A_Concise_Introduction_to_Reinforcement_- Learning https://doi.org/10.13140/RG.2.2.31027.53285

[15]. Wiering, M., Van Hasselt, H., Pietersma, A.-D., & Schomaker, L. (2011). Reinforcement learning algorithms for solving classification problems. Institute of Electrical and Electronics Engineers. https://doi.org/10.1109/ ADPRL.2011.5967372.

[16]. Comaniciu, D. and Meer, P., 2002. Mean shift : A robust approach toward feature space analysis. IEEE Transactions on pattern analysis and machine intelligence 24(5), pp. 603–619

[17]. Orny, C., Chehata, N., Boukir, S. and Guyon, D., 2010. Characterization of maritime pine forest structure changes with vhr satellite imagery: application to the 24th january 2009 windfall damages cartography. Technical report, CNES.

[18]. Cucchi, V., Meredieu, C., Strokes, A., Coligny, F., Suarez, J. and Gardiner, B., 2005. Modelling the windthrow risk for simulated forest stands of maritime pine (pinus pinaster ait.). Forest Ecology and Management 213, pp. 84–196

[19]. Schwarz, M., Steinmeier, C. and Waser, L., 2001. Detection of storm losses in alpine forest areas by different methodic approaches using high resolution satellite data. In: Proceedings of the 21st EARSeL Symposium: Observing our Environment from Space: New Solutions for a New Millenium, pp. 251–257.

[20]. K.R. Gite· Praveen Gupta (2022) GAN-FuzzyNN: Optimization Based Generative Adversarial Network and Fuzzy Neural Network Classification for Change Detection in Satellite Images, Sensing and Imaging (2023) 24:1 https://doi.org/10.1007/s11220-022-00404-3

[21]. Vinod Sapkal, Praveen Gupta (2023) ConvNet Based Malicious URL Identification for Safer Use, Department of Computer Science and Engineering, CSMU, Navi Mumbai, Panvel 410221, India, https://doi.org/10.18280/ria.370230.